

Control of the Morphology and Crystallinity of a PbI_2 Layer for Large-Area Perovskite Films Prepared by Close Space Sublimation

Enrique Pérez-Gutiérrez,^{*,†} M. Judith Percino,^{†,‡} Diana Marcela Montoya,[‡] Diego Solis-Ibarra,[§] Margarita Cerón,[†] and Oracio Barbosa-García[‡]

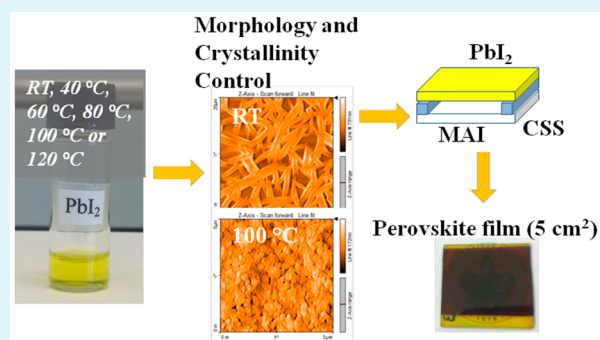
[†]Unidad de Polímeros y Electrónica Orgánica, Instituto de Ciencias, Benemérita Universidad Autónoma de Puebla, Val3-Ecocampus Valsequillo, Independencia O2 Sur 50, San Pedro Zacachimalpa, C.P. 72960 Puebla, México

[‡]Research Group of Optical Properties of Materials (GPOM), Centro de Investigaciones en Óptica A. P. 1-948, 37150 León Guanajuato, Mexico

[§]Laboratorio de Físicoquímica y Reactividad de Superficies (LaFREs), Instituto de Investigaciones en Materiales, Universidad Nacional Autónoma de México, Coyoacán (CDMX) 04510, México

ABSTRACT: In this work, homogeneous PbI_2 films were prepared by the spin-coating technique from PbI_2 -DMF solutions heated at temperatures ranging from room temperature to 120 °C. The homogeneity and morphology of the films change according to the used temperature of solution and are related to the size and distribution of PbI_2 grains; the best crystallinity was observed when PbI_2 solution was preheated at 100 °C. Lead halide perovskite films were prepared by close space sublimation of $\text{CH}_3\text{NH}_3\text{I}$ over the prepared PbI_2 films, and the area of the deposited films was 5 cm². The transformation of PbI_2 into perovskite was carried out at 100 °C under a pressure of -0.8 bar. A remarkable issue reported here is that, by controlling the morphology of the PbI_2 layer with the temperature of PbI_2 -DMF solutions, the final features of MAPbI_3 films can be controlled without requiring extra treatment. Therefore, the device with the best performance, out of a set fabricated with architecture ITO/PEDOT:PSS/perovskite/ PC_{71}BM /cathode, corresponded to the PbI_2 film deposited at 100 °C. This device reached an efficiency of 8.7%. As a cathode, an eutectic alloy of Bi:In:Sn with a melting point of 65 °C was easily deposited without the use of high vacuum. Thus, this work describes a practical way to fabricate perovskite solar cells with efficiencies up to 8.7%.

KEYWORDS: perovskite solar cells, close space sublimation, PbI_2 films, PbI_2 thermal annealing, PbI_2 crystallinity, PbI_2 -DMF adducts, large-area perovskite films



INTRODUCTION

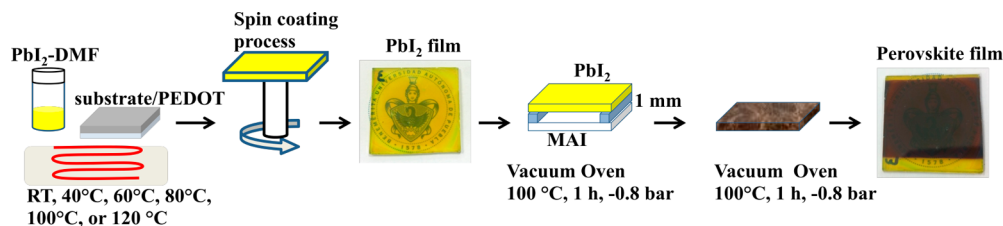
Lead halide perovskite solar cells are an exciting and expanding area of photovoltaic research, and the power conversion efficiency of these hybrid devices has increased from 3.8% to a certified 22.7% in less than 10 years.^{1,2} Intense research has not only focused on efficiency improvements but also on increased stability,^{3,4} device area, and scalability.^{5–7} In particular, the quality of perovskite films, a crucial factor for device performance, is heavily affected by the scaling up of the film area and depends on the deposition method. Several approaches to improving this quality have been reported for the common methods: one-step spin-coating,^{8,9} sequential deposition,^{10,11} co-evaporation,^{12,13} or vapor-assisted deposition.^{14–17} For some vapor-assisted methods, the PbI_2 films can be deposited by spin-coating to achieve good crystallinity and homogeneity. Subsequently, $\text{CH}_3\text{NH}_3\text{I}$ (MAI) can be sublimated in a close space to react with the predeposited PbI_2 layer. Close space sublimation (CSS) has been used to prepare efficient, large-area perovskite films.^{18,19} Li and co-workers¹⁸

report the fabrication of perovskite films as large as 25 cm² by closed space vapor transport. The PbI_2 film was deposited by spin-coating from a DMF solution heated at 75 °C; the $\text{CH}_3\text{NH}_3\text{I}$ vapor, generated under an N_2 atmosphere (2.5 mbar) at 160 °C, reacts with the PbI_2 layer heated at 150 °C. For $\text{CH}_3\text{NH}_3\text{PbI}_3$ (MAPbI_3)-based devices, Li et al.¹⁸ report an efficiency of 14% for an active area of 1 cm², which highlights an easy and low-cost method for preparing large-area films. Also, Guo et al.¹⁹ reported the use of the CSS method for the deposition of 1 cm² perovskite films. In this case, the PbI_2 films were deposited by spin-coating at room temperature (RT), but the sublimation of MAI was carried out at 150 °C under a pressure of -1 bar over 2.5 h to achieve an efficiency of 10.8% for devices with 1 cm² active area.

Received: April 18, 2018

Accepted: July 10, 2018

Published: July 10, 2018

Scheme 1. Representative Scheme for the Preparation of Perovskite Films by Close Space Sublimation^a

^aPbI₂ films are deposited from a solution heated at various temperatures. MAI sublimation was carried out in a vacuum oven at 100 °C and -0.8 bar for 1 h. Logo used with permission from The Autonomous University of Puebla.

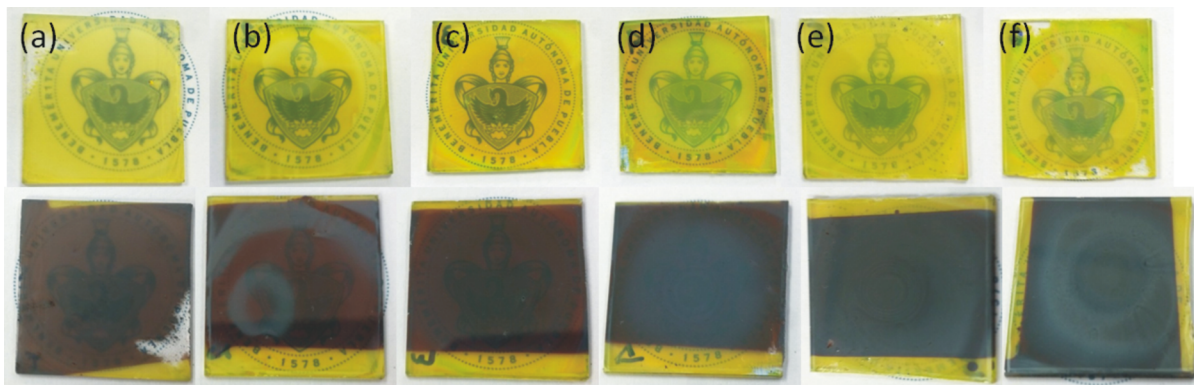


Figure 1. PbI₂ films deposited by heating both substrate and PbI₂-DMF solution at (a) room temperature, (b) 40 °C, (c) 60 °C, (d) 80 °C, (e) 100 °C, and (f) 120 °C, as well as the corresponding perovskite films obtained after close space sublimation of MAI onto PbI₂. Logo used with permission from The Autonomous University of Puebla.

Most of the reports on the CSS method for preparing perovskite layers do not take into account the effect of temperature on the deposition of the PbI₂ layer nor do they consider the temperature used in its transformation into MAPbI₃. For PbI₂, the stacking of a layer of Pb atoms between I atoms could lead to many structures, known as polytypes, which can be produced as a function of thermal treatment.²⁰ The simplest polytype is the 2H phase, with an ABC stacking that is stable at room temperature; however, polytypes 4H and 12R can be formed at 150 and 170 °C, respectively.^{21,22} Furthermore, the high temperatures used for MAI sublimation in CSS could have an effect, not only on the phase of PbI₂ layer but also on the perovskite itself. Recent reports on the thermal stability of CH₃NH₃PbI₃ confirmed that decomposition of the organic material occurs at temperatures higher than 120 °C.^{23,24} The induced decomposition of methylammonium iodide would lead to the formation of HI and CH₃NH₂, which disturb the photovoltaic processes.²⁴ The study of the stability and performance of MAPbI₃ perovskite solar cells conducted by Dualeh et al.²³ showed a decrease in efficiency for devices annealed over 120 °C. At this temperature, the X-ray diffraction patterns showed the characteristic peaks assigned to PbI₂. Furthermore, an efficiency of 11.6% for devices treated at 100 °C decreases to 9.6% when annealed at 150 °C and 8.5% at 175 °C.

In this work, PbI₂ films of 5 cm² were deposited by spin-coating and six temperatures, from room temperature (RT) to 120 °C, were used for preheating the PbI₂-DMF solutions. The morphology and quality of the films showed the strong influence of the PbI₂-DMF solutions temperature used, which changes the size and distribution of the PbI₂ grain. MAPbI₃ perovskite films were prepared by the close space sublimation method, where the reaction between the PbI₂ films and

CH₃NH₃I vapor was achieved in a vacuum oven under a pressure of -0.8 bar at just 100 °C. The morphology of the perovskite layer was determined thus by the morphology of the PbI₂ film. The XRD pattern for PbI₂ and the perovskite films showed higher crystallinity and homogeneity when PbI₂-DMF solution was preheated at 100 °C, and a better photovoltaic performance was recorded. Devices with architecture ITO/PEDOT:PSS/perovskite/PC₇₁BM/cathode were prepared. As a cathode, an eutectic alloy of Bi:In:Sn, known as Field's metal, with a melting point of 65 °C, was easily deposited without the use of high vacuum. Field's metal has been previously reported by the authors²⁵⁻²⁷ to be an effective cathode in organic solar cells. Devices where PbI₂ was deposited from a solution at 100 °C showed the best performance, with an efficiency of 8.7%.

EXPERIMENTAL SECTION

Materials. Lead iodide and PC₇₁BM were purchased from Aldrich, and methylamine iodide was synthesized according to previous reports.²⁸ PEDOT:PSS (Clevios PVP AI4083) was obtained from Heraeus-Clevios. All solvents were acquired from Sigma-Aldrich and used as received. As substrate device, ITO/glass with 10–15 Ω/□ was acquired from Delta Technologies.

Film Deposition and Device Fabrication. The glass and ITO/glass substrates were cleaned with ethanol in an ultrasonic bath and rubbed with alcohol-wetted cotton. After that, the substrates were dried with clean and dry air and kept at 85 °C over 12 h. A first layer of PEDOT:PSS was spin-coated onto the substrates and annealed at 120 °C for 15 min in air. PbI₂ films were deposited by spin-coating from a solution with DMF as solvent, with a concentration of 300 mg/mL. The temperatures of PbI₂-DMF solutions used for deposition were as follows: room temperature, 40 °C, 60 °C, 80 °C, 100 °C, and 120 °C. In all cases the solution and substrate were kept on a hot plate for 20 min before deposition. All the PbI₂ films were then annealed at 85 °C in a vacuum. Several batches of films were prepared from one solution

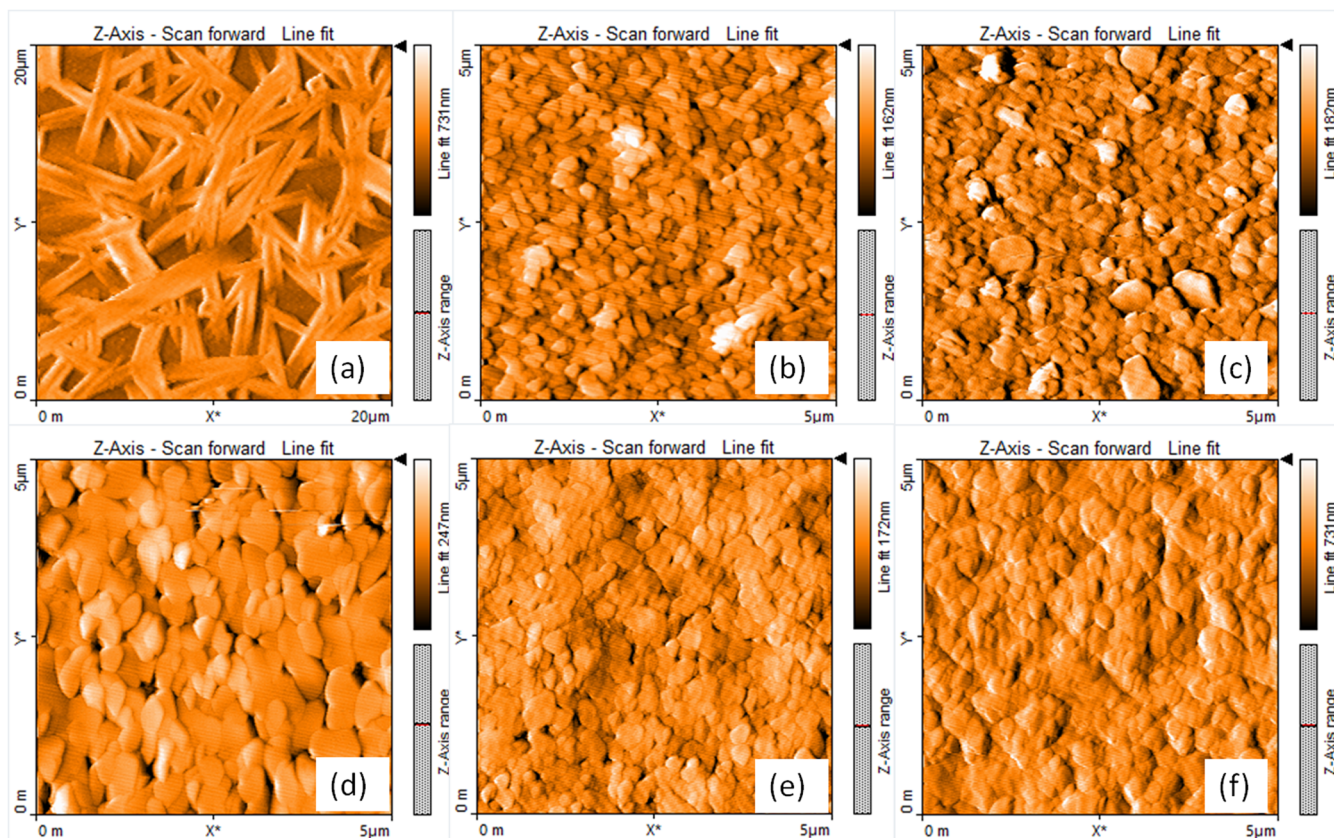


Figure 2. AFM images for PbI_2 films deposited by heating both substrate and solution at (a) room temperature, (b) 40 °C, (c) 60 °C, (d) 80 °C, (e) 100 °C, and (f) 120 °C.

and from at least two solutions more to ensure the reproducibility of experiments.

The MAI film was deposited using a solution of 30 mg/mL with isopropyl alcohol as solvent, the glass substrate was heated on a hot plate at 50 °C, and 200 μL of solution was deposited on the substrate. After IPA evaporation, a transparent and homogeneous film was obtained. For transformation into perovskite material, PbI_2 and MAI films were placed face-to-face and separated by 1 mm (glass substrate). The films were collocated on a vacuum oven under a pressure of -0.8 bar and heated at 100 °C by 1 h. After the transformation, perovskite films were heated under the same pressure and temperature conditions to eliminate excess MAI. The procedure is represented in Scheme 1.

For photovoltaic devices, a PC_{71}BM film (100 nm) was deposited on top of the perovskite film under normal room conditions. Finally, the melted cathode (eutectic alloy Field's metal) was dropped on top of the masked devices heated at 80 °C. The active area was 0.07 cm^2 .

Characterization and Measurements. The morphology and thickness were analyzed using atomic force microscopy (AFM) with the microscope EasyScan2 from Nanosurf operating in contact mode under ambient conditions. This has a maximum square scanning area of 110 μm^2 . A solar simulator (Sciencetech SS150) was used for device characterization. The light intensity was calibrated to 100 mW/cm^2 using an Oriel reference cell. The I - V curves were recorded with a Keithley 2450 SourceMeter under normal atmosphere. Powder XRD analysis was conducted using a Bruker D2 Phaser diffractometer, with $\text{Cu K}\alpha$ (1.54060 Å).

RESULTS AND DISCUSSION

The temperature of solution used for deposition of the PbI_2 films strongly affected the homogeneity of films over substrates (top pictures in Figure 1). Films deposited from solutions either at room temperature or 100 °C were homogeneous but

opaque, whereas the films deposited from solutions at 60 °C were homogeneous and transparent. On the other hand, when solutions were heated at 40, 80, and 120 °C, the deposited films showed clear and opaque areas that were more evident after the transformation of PbI_2 into $\text{CH}_3\text{NH}_3\text{PbI}_3$ by CSS of MAI (see bottom pictures in Figure 1).

These differences in the films shown in Figure 1 are due to the size and distribution of the PbI_2 grains, as revealed by AFM analysis (Figure 2). In this case, they could have occurred due to a temperature gradient generated by the initial temperature of the substrate and solution and the rapid freezing by the spin process. The well-known needle morphology for PbI_2 was observed for films deposited at room temperature; meanwhile, a granular morphology was obtained by heating the same solution (and substrate). The grain size and the average roughness varied. In particular, the average roughness for the films was 10.4, 11.0, 16.2, 12.4, and 25.3 nm for temperatures 40, 60, 80, 100, and 120 °C, respectively. Also the films' thicknesses changed owing to the used temperature; for films deposited at room temperature the average thickness was 288 nm while for films deposited from a solution at 120 °C the average thickness was 324 nm. It can be observed that the grain size for films deposited from solutions at 80 °C are larger compared with other deposition temperatures. This could be due to the formation of PbI_2 -DMF adducts, as has been previously reported by Wakamiya et al.²⁸ Using single-crystal X-ray diffraction, they observed one DMF molecule coordinated to Pb to form one-dimensional structures. Also, by thermogravimetric analysis, they showed that the release of coordinated DMF started around 70 °C and was completed at 112.6 °C. This occurred when the samples changed from pale

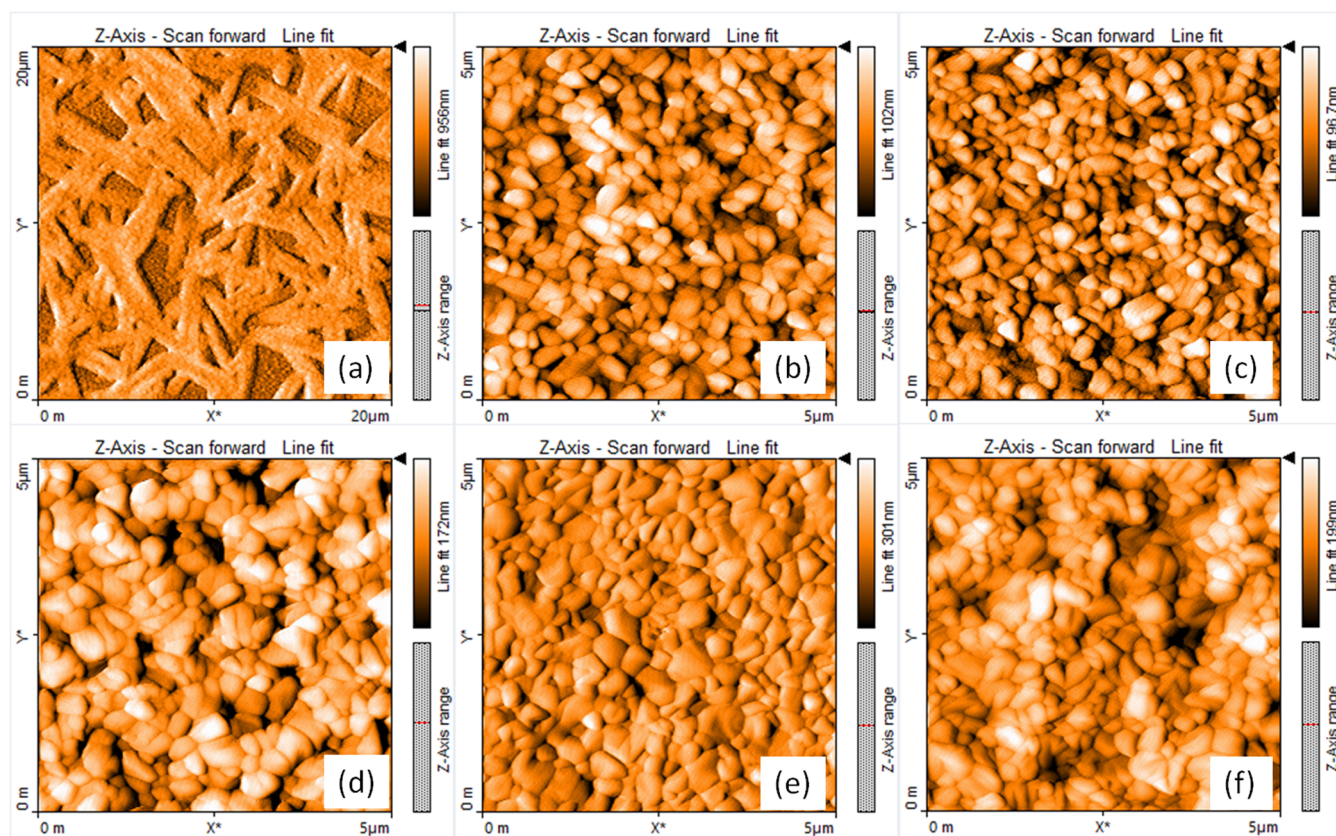


Figure 3. AFM images for perovskite films obtained by close space sublimation of MAI onto PbI_2 films. PbI_2 was deposited by spin-coating from solutions at (a) room temperature, (b) 40 °C, (c) 60 °C, (d) 80 °C, (e) 100 °C, and (f) 120 °C.

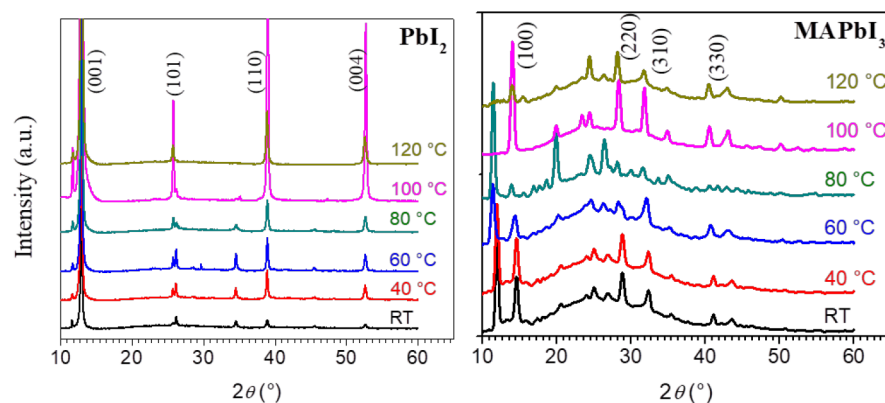


Figure 4. XRD patterns for PbI_2 films deposited from solutions heated at several temperatures and transformed into MAPbI_3 by close space sublimation.

to deep yellow. The results reported here are consistent with their report. Our films changed color from pale to strong yellow as the temperature for deposition increased. A competition between pure PbI_2 grains and adduct grains could be the reason for the morphology in the films deposited at 80 °C.

The observed morphology on PbI_2 films affects the final morphology of the perovskite material (Figure 3). For the case when PbI_2 was deposited from a heated solution, the perovskite films showed granular morphology, but the grain size changed. When the PbI_2 films were deposited by heated solutions at 40 or 60 °C, a similar grain size was obtained; meanwhile, different sizes were obtained for higher temperatures. The perovskite films were more compact when solution

was heated at 100 °C, but some pinholes showed up when the solution was at 120 °C. Changes in morphology for MAPbI_3 films deposited from DMF solution were previously reported, and these were related to the low solubility of PbI_2 and to the high rate of solvent evaporation in the spin-coating process.²⁹ To improve the quality of MAPbI_3 films, co-solvents such as DMSO or γ -butyrolactone were used. Also, a solvent procedure was reported that controls both homogeneity and grain size; this was implemented in a washing procedure with a nonpolar solvent such as diethyl ether, chlorobenzene, or toluene.^{29,30}

The above-mentioned studies on the control of the grain size and morphology for perovskite films showed the strong influence of these parameters on the final performance of solar

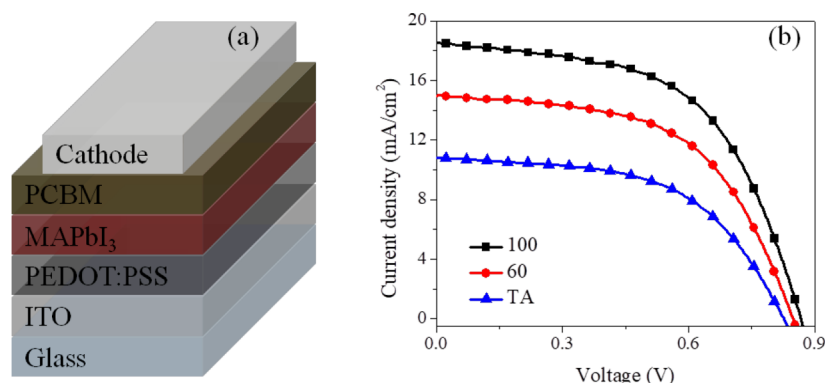


Figure 5. (a) Schematic representation of the solar cell architecture and (b) J - V curves for the best perovskite photovoltaic devices obtained from PbI_2 films deposited from solutions at room temperature (TA), 60 and 100 °C.

cells. Homogeneous and quality films are necessary to obtain the optimal photovoltaic parameters for the devices. In our case, the temperature for the deposition of PbI_2 films was implemented to avoid the use of an additional solvent, and this procedure simplifies the process. The final average thickness for perovskite films was 340 and 365 nm for films deposited at RT and from a solution at 120 °C, respectively.

The crystallinity of PbI_2 and perovskite films was analyzed by XRD, and Figure 4 shows the pattern for PbI_2 films. The predominant diffraction peaks for planes 001, 101, 110, and 004 can be seen,^{31–33} and no evidence for peaks related to 4H or 12R polytypes is observed.²² However, a reflection appears at 11.7° that would be due to the formation of $\text{PbI}_2\cdot\text{DMF}$ adducts that have been previously reported and mentioned above.^{28,34,35} Manser et al.³⁴ reported for PbI_2 films the (001) plane at 12.7° (2θ), but also a lower angle reflection indicating larger lattice spacing in the structure. They relate this peak to an expansion in the lattice as a result of incorporation of some combination of methylammonium cations and DMF molecules between the inorganic sheets. With the CSS process, it could be expected that the substitution of a DMF molecule in $\text{PbI}_2\cdot\text{DMF}$ by $\text{CH}_3\text{NH}_3\text{I}$ will form $\text{CH}_3\text{NH}_3\text{PbI}_3$. The XRD patterns for perovskite showed peaks corresponding to (100), (220), (310), and (330);^{36,37} however, when PbI_2 was deposited at 40, 60, and 80 °C, the reflection peak at 11.7° (2θ) was observed. This peak shows that some adducts remain in the perovskite lattice after the sublimation of MAI. On the other hand, the perovskite films obtained from PbI_2 film deposited at 100 and 120 °C do not show that peak, indicating the total transformation of PbI_2 into perovskite material. For perovskite films obtained from PbI_2 deposited from solution at 80 °C, the XRD pattern showed high intensity for peaks at 11.7° (2θ) and 20° (2θ) assigned to $\text{PbI}_2\cdot\text{DMF}$ adducts and MAI, respectively.³⁴ As mentioned above, Wakamiya et al.²⁸ reported that $\text{PbI}_2\cdot\text{DMF}$ adducts start to release near 80 °C. This temperature applied in the deposition of PbI_2 films could stimulate the formation of a bigger amount of $\text{PbI}_2\cdot\text{DMF}$ adducts. The bigger amount of adducts could be a detriment to the reaction between PbI_2 and MAI, and this could be the reason for the observed peak at 20° (2θ).

To evaluate how these films would behave in a photovoltaic device, we fabricated devices using the PbI_2 films produced from solutions at RT, 60 °C, and 100 °C. For that purpose, we assembled devices with architecture ITO/PEDOT:PSS/perovskite/PCBM/FM (where FM is a low melting point eutectic alloy of Bi:In:Sn, commonly known as Field's metal); a

schematic representation for the devices' architecture is shown in Figure 5. The electrical parameters of such devices are summarized in Table 1. The best performance was for the

Table 1. Parameters for Perovskite Photovoltaic Devices, With Three Temperatures for the Deposition of PbI_2 Films^a

temp of $\text{PbI}_2\cdot\text{DMF}$ solution	V_{oc} (mV)	J_{sc} (mA/cm ²)	FF	η (%)
RT	829 ± 4	14.3 ± 0.6	0.40 ± 0.02	4.88 ± 0.4
60 °C	848 ± 5	14.9 ± 0.5	0.55 ± 0.01	7.05 ± 0.4
100 °C	867 ± 4	18.5 ± 0.3	0.54 ± 0.01	8.70 ± 0.2

^aAverage values determined from eight devices along with standard deviations.

device where the PbI_2 was deposited at 100 °C. An efficiency of 8.7% was obtained with a V_{oc} of 867 mV, J_{sc} of 18.5 mA/cm², and FF of 0.54 (Figure 5). The improved performance for such devices, related to the higher J_{sc} , could be directly associated with the better morphology obtained at this temperature. As mentioned in the literature, the use of additives or washing solvents induces the formation of extremely flat and dense films with a direct impact on photocurrent.^{30,31} The increase in current is assigned to the lower loss of photogenerated charge carriers in the grain boundaries and recombination processes. The role of additives and solvents is to control the rapid reaction between MAI and PbI_2 , which enables the formation of highly uniform and dense surfaces. The remarkable achievement in our case is that, by controlling the morphology of the PbI_2 layer with the temperature of solutions used for its deposition, the final features of MAPbI_3 films can be determined without the use of extra solvents. Also, the temperature improves the crystallinity and avoids the formation of the $\text{PbI}_2\cdot\text{DMF}$ complex.

Despite the higher efficiencies reported by other authors for devices prepared by CSS, in our case, all of the films were deposited at normal room conditions without the use of a controlled atmosphere and with an alternative cathode.

CONCLUSIONS

Homogeneous films of PbI_2 can be deposited over large areas by spin-coating from heated solutions, and this helps to control the distribution and size of PbI_2 grains. The films thus deposited were transformed into MAPbI_3 by close space sublimation. XRD analysis showed the presence of $\text{PbI}_2\cdot\text{DMF}$ adducts that remain after transformation of PbI_2 into

perovskite when the PbI_2 films were deposited from solutions at temperatures below 100 °C. When the solution and substrates for the deposition of PbI_2 are heated at 100 °C, a homogeneous and dense film of PbI_2 and then perovskite can be achieved over large areas without the presence of DMF adducts. The improvement in the quality of perovskite film influences the photovoltaic devices, and an efficiency of 8.7% was obtained from devices prepared in a normal atmosphere with architecture ITO/PEDOT:PSS/perovskite/ PC_{71}BM /cathode.

AUTHOR INFORMATION

Corresponding Author

*E-mail: enrique.pgutierrez@correo.buap.mx.

ORCID

M. Judith Percino: 0000-0003-1610-7155

Notes

The authors declare no competing financial interest.

ACKNOWLEDGMENTS

We express our gratitude to CATEDRAS-CONACYT and VIEP-BUAP (Project PEZM-NAT16-G and Project COL528150-VIEP2018).

REFERENCES

- (1) Kojima, A.; Teshima, K.; Shirai, Y.; Miyasaka, T. Organometal Halide Perovskites as Visible–Light Sensitizers for Photovoltaic Cells. *J. Am. Chem. Soc.* **2009**, *131*, 6050.
- (2) *Best Research Cell Efficiencies*; U.S. National Renewable Energy Laboratory (NREL), 2017; <https://www.nrel.gov/pv/assets/images/efficiency-chart.png> (accessed Jun. 1, 2018).
- (3) Grätzel, M. The Rise of Highly Efficient and Stable Perovskite Solar Cells. *Acc. Chem. Res.* **2017**, *50*, 487–491.
- (4) Grancini, G.; Roldán-Carmona, C.; Zimmermann, I.; Mosconi, E.; Lee, X.; Martineau, D.; Nabey, S.; Oswald, F.; De Angelis, F.; Graetzel, M.; Nazeeruddin, M. K. One-Year Stable Perovskite Solar Cells by 2D/3D Interface Engineering. *Nat. Commun.* **2017**, *8*, 15684.
- (5) Chen, H.; Ye, F.; Tang, W.; He, J.; Yin, M.; Wang, Y.; Xie, F.; Bi, E.; Yang, X.; Grätzel, M.; Han, L. A Solvent–and Vacuum–Free Route to Large–Area Perovskite Films for Efficient Solar Modules. *Nature* **2017**, DOI: 10.1038/nature23877.
- (6) Lee, J.; Kang, H.; Kim, G.; Back, H.; Kim, J.; Hong, S.; Park, B.; Lee, E.; Lee, K. Achieving Large–Area Planar Perovskite Solar Cells by Introducing an Interfacial Compatibilizer. *Adv. Mater.* **2017**, *29*, 1606363.
- (7) Mali, S. S.; Kim, H.; Kim, H. H.; Park, G. R.; Shim, S. E.; Hong, C. K. Large Area, Waterproof, Air Stable and Cost Effective Efficient Perovskite Solar Cells Through Modified Carbon Hole Extraction Layer. *Mater. Today Chem.* **2017**, *4*, 53–63.
- (8) Li, C.; Guo, Q.; Qiao, W.; Chen, Q.; Ma, S.; Pan, X.; Wang, F.; Yao, J.; Zhang, C.; Xiao, M.; Dai, S.; Tan, Z. Efficient Lead Acetate Sourced Planar Heterojunction Perovskite Solar Cells with Enhanced Substrate Coverage Via One–Step Spin–Coating. *Org. Electron.* **2016**, *33*, 194–200.
- (9) Zhang, W.; Saliba, M.; Moore, D. T.; Pathak, S. K.; Hörantner, M. T.; Stergiopoulos, T.; Stranks, S. D.; Eperon, G. E.; Alexander-Webber, J. A.; Abate, A.; Sadhanala, A.; Yao, S.; Chen, Y.; Friend, R. H.; Estroff, L. A.; Wiesner, U.; Snaith, H. J. Ultrasoft Organic–Inorganic Perovskite Thin–Film Formation and Crystallization for Efficient Planar Heterojunction Solar Cells. *Nat. Commun.* **2015**, *6*, 6142.
- (10) Xi, J.; Wu, Z.; Dong, H.; Xia, B.; Yuan, F.; Jiao, B.; Xiao, L.; Gong, Q.; Hou, X. Controlled Thickness and Morphology for Highly Efficient Inverted Planar Heterojunction Perovskite Solar Cells. *Nanoscale* **2015**, *7*, 10699–10707.
- (11) Lewis, A. E.; Zhang, Y.; Gao, P.; Nazeeruddin, M. K. Unveiling the Concentration-Dependent Grain Growth of Perovskite Films from One– and Two–Step Deposition Methods: Implications for Photovoltaic Application. *ACS Appl. Mater. Interfaces* **2017**, *9*, 25063–25066.
- (12) Ono, L. K.; Leyden, M. R.; Wang, S.; Qi, Y. Organometal Halide Perovskite Thin Films and Solar Cells by Vapor Deposition. *J. Mater. Chem. A* **2016**, *4*, 6693–6713.
- (13) Ng, A.; Ren, Z.; Shen, Q.; Cheung, S. H.; Gokkaya, H. C.; Bai, G.; Wang, J.; Yang, L.; So, S. K.; Djurišić, A. B.; Leung, W. W.–F.; Hao, J.; Chan, W. K.; Surya, C. Efficiency Enhancement by Defect Engineering in Perovskite Photovoltaic Cells Prepared Using Evaporated $\text{PbI}_2/\text{CH}_3\text{NH}_3\text{I}$ Multilayers. *J. Mater. Chem. A* **2015**, *3*, 9223–9231.
- (14) Conings, B.; Brette, S. A.; Babayigit, A.; Gauquelin, N.; Cardinaletti, I.; Manca, J.; Verbeeck, J.; Snaith, H. J.; Boyen, H.–G. Structure–Property Relations of Methylamine Vapor Treated Hybrid Perovskite $\text{CH}_3\text{NH}_3\text{PbI}_3$ Films and Solar Cells. *ACS Appl. Mater. Interfaces* **2017**, *9*, 8092–8099.
- (15) Tavakoli, M. M.; Gu, L.; Gao, Y.; Reckmeier, C.; He, J.; Rogach, A. L.; Yao, Y.; Fan, Z. Fabrication of Efficient Planar Perovskite Solar Cells Using a One–Step Chemical Vapor Deposition Method. *Sci. Rep.* **2015**, *5*, 14083.
- (16) Zhang, T.; Guo, N.; Li, G.; Qian, X.; Li, L.; Zhao, Y. A general non- $\text{CH}_3\text{NH}_3\text{X}$ ($\text{X} = \text{I}, \text{Br}$) one-step deposition of $\text{CH}_3\text{NH}_3\text{PbX}_3$ perovskite for high performance solar cells. *J. Mater. Chem. A* **2016**, *4*, 3245–3248.
- (17) Zhang, T.; Guo, N.; Li, G.; Qian, X.; Zhao, Y. A controllable fabrication of grain boundary PbI_2 nanoplates passivated lead halide perovskites for high performance solar cells. *Nano Energy* **2016**, *26*, 50–56.
- (18) Li, G.; Ho, J. Y. L.; Wong, M.; Kwok, H.–S. Low Cost, High Throughput and Centimeter–Scale Fabrication of Efficient Hybrid Perovskite Solar Cells by Closed Space Vapor Transport. *Phys. Status Solidi RRL* **2016**, *10*, 153–157.
- (19) Guo, Q.; Li, C.; Qiao, W.; Ma, S.; Wang, F.; Zhang, B.; Hu, L.; Dai, S.; Tan, Z. The Growth of a $\text{CH}_3\text{NH}_3\text{PbI}_3$ Thin Film Using Simplified Close Space Sublimation for Efficient and Large Dimensional Perovskite Solar Cells. *Energy Environ. Sci.* **2016**, *9*, 1486.
- (20) Beckmann, P. A. A Review of Polytypism in Lead Iodide. *Cryst. Res. Technol.* **2010**, *45*, 455–460.
- (21) Konings, R. J. M.; Cordfunke, E. H. R.; van der Laan, R. R. Enthalpy Increment Measurements of PbI_2 : Evidence for a Reversible Polytypic Transition. *J. Alloys Compd.* **1995**, *230*, 85–88.
- (22) Flahaut, E.; Sloan, J.; Friedrichs, S.; Kirkland, A. I.; Coleman, K. S.; Williams, V. C.; Hanson, N.; Hutchison, J. L.; Green, M. L. H. Crystallization of 2H and 4H PbI_2 in Carbon Nanotubes of Varying Diameters and Morphologies. *Chem. Mater.* **2006**, *18*, 2059–2069.
- (23) Dualeh, A.; Tétreault, N.; Moehl, T.; Gao, P.; Nazeeruddin, M. K.; Grätzel, M. Effect of Annealing Temperature on Film Morphology of Organic–Inorganic Hybrid Perovskite Solid-State Solar Cells. *Adv. Funct. Mater.* **2014**, *24*, 3250–3258.
- (24) Dualeh, A.; Gao, P.; Seok, S. I.; Nazeeruddin, M. K.; Grätzel, M. Thermal Behavior of Methylammonium Leadtrihalide Perovskite Photovoltaic Light Harvesters. *Chem. Mater.* **2014**, *26*, 6160–6164.
- (25) Pérez-Gutiérrez, E.; Barreiro-Argüelles, D.; Maldonado, J.–L.; Meneses-Nava, M.–A.; Barbosa-García, O.; Ramos-Ortiz, G.; Rodríguez, M.; Fuentes-Hernández, C. Semiconductor Polymer/Top Electrode Interface Generated by Two Deposition Methods and Its Influence on Organic Solar Cell Performance. *ACS Appl. Mater. Interfaces* **2016**, *8*, 28763–28770.
- (26) Pérez-Gutiérrez, E.; Lozano, J.; Gaspar-Tánori, J.; Maldonado, J.–L.; Gómez, B.; López, L.; Amores-Tapia, L.–F.; Barbosa-García, O.; Percino, M.–J. Organic Solar Cells all Made by Blade and Slot–Die Coating Techniques. *Sol. Energy* **2017**, *146*, 79–84.
- (27) Barreiro-Argüelles, D.; Ramos-Ortiz, G.; Maldonado, J.–L.; Pérez-Gutiérrez, E.; Romero-Borja, D.; Álvarez-Fernández, A. PTB7:PC71BM-Based Solar Cells Fabricated with the Eutectic

Alloy Field's Metal as an Alternative Cathode and the Influence of an Electron Extraction Layer. *IEEE J. Photovolt.* **2017**, *7*, 191–198.

(28) Wakamiya, A.; Endo, M.; Sasamori, T.; Tokitoh, N.; Ogomi, Y.; Hayase, S.; Murata, Y. Reproducible Fabrication of Efficient Perovskite-based Solar Cells: X-ray Crystallographic Studies on the Formation of $\text{CH}_3\text{NH}_3\text{PbI}_3$ Layers. *Chem. Lett.* **2014**, *43*, 711–713.

(29) Ahn, N.; Son, D.-Y.; Jang, I.-H.; Kang, S. M.; Choi, M.; Park, N.-G. Highly Reproducible Perovskite Solar Cells with Average Efficiency of 18.3% and Best Efficiency of 19.7% Fabricated via Lewis Base Adduct of Lead(II) Iodide. *J. Am. Chem. Soc.* **2015**, *137*, 8696–8699.

(30) Jeon, N. J.; Noh, J. H.; Kim, Y. C.; Yang, W. S.; Ryu, S.; Seok, S. I. Solvent Engineering for High-Performance Inorganic–Organic Hybrid Perovskite Solar Cells. *Nat. Mater.* **2014**, *13*, 897–903.

(31) Caldeira Filho, A. M.; Mulato, M. Characterization of Thermally Evaporated Lead Iodide Films Aimed for the Detection of X-rays. *Nucl. Instrum. Methods Phys. Res., Sect. A* **2011**, *636*, 82–86.

(32) Schieber, M.; Zamoschik, N.; Khakhan, O.; Zuck, A. Structural Changes During Vapor–Phase Deposition of Polycrystalline– PbI_2 Films. *J. Cryst. Growth* **2008**, *310*, 3168–173.

(33) Acuña, D.; Krishnan, B.; Shaji, S.; Sepulveda, S.; Menchaca, J. L. Growth and Properties of Lead Iodide Thin Films by Spin Coating. *Bull. Mater. Sci.* **2016**, *39*, 1453–1460.

(34) Manser, J. S.; Saidaminov, M. I.; Christians, J. A.; Bakr, O. M.; Kamat, P. V. Making and Breaking of Lead Halide Perovskites. *Acc. Chem. Res.* **2016**, *49*, 330–338.

(35) Guo, Y.; Shoyama, K.; Sato, W.; Matsuo, Y.; Inoue, K.; Harano, K.; Liu, C.; Tanaka, H.; Nakamura, E. Chemical Pathways Connecting Lead(II) Iodide and Perovskite via Polymeric Plumbate(II) Fiber. *J. Am. Chem. Soc.* **2015**, *137*, 15907–15914.

(36) Hao, F.; Stoumpos, C. C.; Liu, Z.; Chang, R. P. H.; Kanatzidis, M. G. Controllable Perovskite Crystallization at a Gas–Solid Interface for Hole Conductor–Free Solar Cells with Steady Power Conversion Efficiency over 10%. *J. Am. Chem. Soc.* **2014**, *136*, 16411–16419.

(37) Baikie, T.; Fang, Y.; Kadro, J. M.; Schreyer, M.; Wei, F.; Mhaisalkar, S. G.; Grätzel, M.; White, T. J. Synthesis and Crystal Chemistry of the Hybrid Perovskite $(\text{CH}_3\text{NH}_3)\text{PbI}_3$ for Solid–State Sensitised Solar Cell Applications. *J. Mater. Chem. A* **2013**, *1*, 5628–5641.